Tu, R., Wang, R., Zhang, Y., Walter, T. R. (2014): Application of a net-based baseline correction scheme to strong-motion records of the 2011 Mw 9.0 Tohoku earthquake. - *Geophysical Journal International*, *197*, 3, p. 1808-1821.

DOI: http://doi.org/10.1093/gji/ggu092

Geophysical Journal International

Geophys. J. Int. (2014) **197,** 1808–1821
Advance Access publication 2014 April 3

doi: 10.1093/gji/ggu092

Application of a net-based baseline correction scheme to strong-motion records of the 2011 *M*w 9.0 Tohoku earthquake

Rui Tu, Rongjiang Wang, Yong Zhang and Thomas R. Walter

*GFZ German Research Centre for Geosciences, Telegrafenberg, D-*14473 *Potsdam, Germany. E-mail: wang@gfz-potsdam.de*

Accepted 2014 March 10. Received 2014 March 10; in original form 2013 September 9

SUMMARY

The description of static displacements associated with earthquakes is traditionally achieved using GPS, EDM or InSAR data. In addition, displacement histories can be derived from strong-motion records, allowing an improvement of geodetic networks at a high sampling rate and a better physical understanding of earthquake processes. Strong-motion records require a correction procedure appropriate for baseline shifts that may be caused by rotational motion, tilting and other instrumental effects. Common methods use an empirical bilinear correction on the velocity seismograms integrated from the strong-motion records. In this study, we overcome the weaknesses of an empirically based bilinear baseline correction scheme by using a net-based criterion to select the timing parameters. This idea is based on the physical principle that low-frequency seismic waveforms at neighbouring stations are coherent if the interstation distance is much smaller than the distance to the seismic source. For a dense strong-motion network, it is plausible to select the timing parameters so that the correlation coefficient between the velocity seismograms of two neighbouring stations is maximized after the baseline correction. We applied this new concept to the KiK-Net and K-Net strong-motion data available for the 2011 *M*w 9.0 Tohoku earthquake. We compared the derived coseismic static displacement with high-quality GPS data, and with the results obtained using empirical methods. The results show that the proposed net-based approach is feasible and more robust than the individual empirical approaches. The outliers caused by unknown problems in the measurement system can be easily detected and quantified.

Key words: Earthquake ground motions.

1 INTRODUCTION

Transient and permanent ground displacements associated with tectonic earthquakes provide important information for identifying active seismogenic faults, reconstructing the kinematic source process of earthquakes, or predicting post-seismic processes based on modelling (McComb *et al.* 1943; Graizer 1979; Chiu 1997; Zhu 2003). Static ground displacement data are typically obtained using traditional and modern geodetic methods, such as the levelling, GPS and InSAR techniques (Larson *et al.* 2003; Salichon *et al.* 2003; Bock & Prawirodirdjo 2004; Delouis *et al.* 2010; Irwan *et al.* 2011). Many papers have shown the importance of GPS coseismic displacement to analyse the source and early response, especially for the 2011 Tohoku earthquake (Ohta *et al.* 2012; Wright *et al.* 2012; Colombelli *et al.* 2013; Melgar *et al.* 2013; Wang *et al.* 2013). Recent studies have shown that near-field ground velocity and displacement histories cannot be fully analysed using these geodetic methods because of the difficulty in obtaining data in real time (in the case of InSAR) or because of the insufficient signal resolution at high frequencies (GPS), which does not allow the quantification of dynamic processes associated with the passage of seismic waves. To overcome this difficulty, many approaches have been proposed recently to jointly use GPS and seismometer measurements (Nikolaidis *et al.* 2001; Emore *et al.* 2007; Bock *et al.* 2011; Geng *et al.* 2013a; Li *et al.* 2013; Melgar *et al.* 2013; Tu *et al.* 2013, 2014; Wang *et al.* 2013).

High-rate continuous GPS networks are still rare, except in a few developed countries, such as Japan. Strong-motion sensors recording ground acceleration, however, are almost ubiquitous around the world. A large strong-motion database is available for many seismically active regions. Previous studies have shown that displacements may be derived from strong-motion records after an appropriate correction for baseline errors of the accelerometer sensor, allowing near real-time and high sampling rates (Iwan *et al.* 1985; Wu & Wu 2007; Chao *et al.* 2009; Wang *et al.* 2011). There are many different empirical methods for the baseline correction. Based on the idea of Iwan *et al.* (1985), a baseline shift of an accelerogram can be composed of (i) a pre-event baseline shift, (ii) a co-event transient

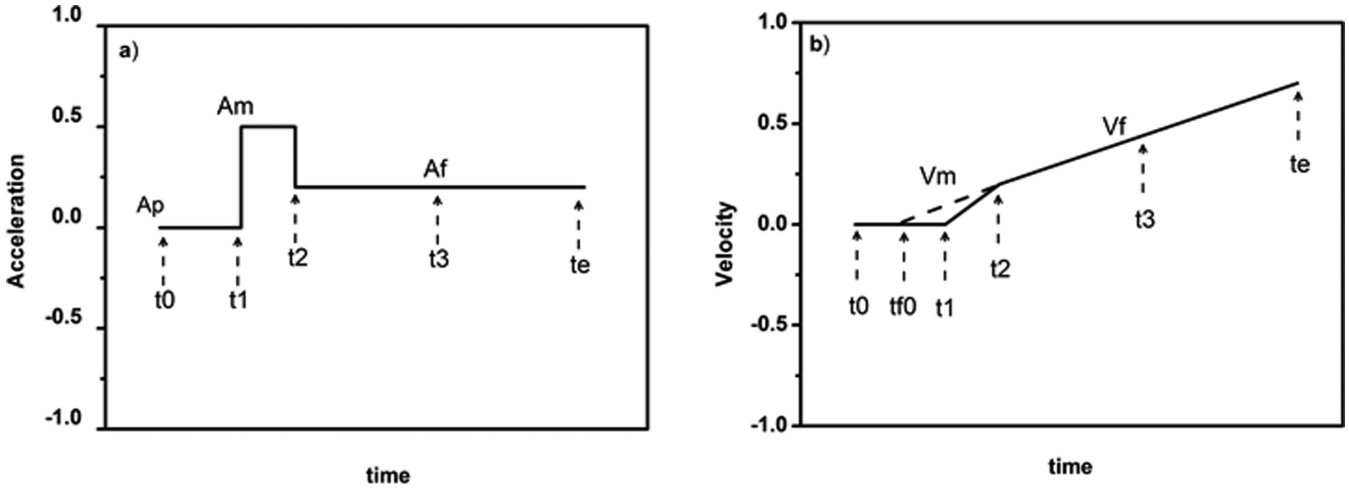

Figure 1. The empirical baseline correction scheme of Iwan *et al.* (1985). (a) The baseline acceleration shift of strong-motion records is generally composed of the pre-event part A_P (here, $A_P = 0$), the average of the transient part A_m and the permanent part A_f. (b) The bilinear trend of the velocity seismogram derived from the baseline acceleration errors. The time parameters used are (t_0, t_e), the time window of the data, (t_1, t_2), the period of the transient baseline shift, t_3, the end of strong ground shaking, t_{f0}, and the zero crossing of the post-event velocity trend.

(dynamic) part associated with the passage of the seismic waves and (iii) a post-event quasi-permanent baseline shift, as shown in Fig. 1.

Iwan *et al.* (1985) assumed that a baseline shift is caused by transducer hysteresis of the measurement system and introduces an average transient baseline offset during the strongest portion of ground shaking ($t_1 \leq t < t_2$) and a remaining permanent baseline offset after the strong ground shaking ($t_1 \geq t_2$). They empirically selected t_1 as the time when the absolute acceleration first exceeded a pre-defined threshold of 50 cm s^{-2}. Two options have been proposed to identify the time t_2, which is selected depending on the final net displacement. In option 1, t_2 characterizes the time after the acceleration never exceeds the pre-defined 50 cm s^{-2} threshold. In option two, t_2 is determined to obtain a minimal final net displacement.

Practice shows, however, that the 50 cm s^{-2} threshold proposed by Iwan *et al.* (1985) is an oversimplification that possibly affects the correct data analysis. Because baseline shifts in strong-motion records are dominantly caused by ground tilt affecting the stability of the station itself (Trifunac & Todorovska 2001a,b; Graizer 2005, 2006), acceleration levels well below 50 cm s^{-2} may be significant. Boore (2001) generalized the method discussed by Iwan *et al.* (1985), allowing t_1 and t_2 to be free parameters. Various choices of t_1 and t_2 can lead to a reasonable velocity history, although large variations in the final displacement were observed (Boore 2001).

Several improvements on the Iwan *et al.* (1985) methods have recently been published based on bilinear correction (Wu & Wu 2007; Chao *et al.* 2009; Wang *et al.* 2011). Recent improvements made on this bilinear correction concept and selection of the time parameters, t_1 and t_2, based on different empirically based criterions (e.g. the displacement–time history after the baseline correction should take a ramp function form) instead of the simple threshold approach, are reviewed in Wang *et al.* (2011). A common limitation of the previous studies is that strong-motion baseline corrections are made independently from station to station. The station-independent correction strategy is potentially associated with large uncertainties in the derived displacement data because local effects and outliers are not discernible. Wang *et al.* (2013) noted that a common problem is that uncertainties can only be quantified by considering an independent geodetic reference, for example, a local GPS network.

In this study, we propose a net-based strategy for an empirical baseline correction, in which maximizing the maximum cross-correlation coefficient between derived low-frequency velocity waveforms of neighbouring stations is used as the criterion for determining the bilinear correction constants. For simplicity, the maximum cross-correlation coefficient is called the correlation throughout this paper. This new approach is particularly useful for the KiK-Net and K-Net in Japan but may be used wherever a dense strong-motion network is available. We demonstrate the feasibility of our net-based strategy for strong-motion data recorded during the 2011 Tohoku earthquake, Japan, and validate it against continuous GPS records. We show that outliers in displacements derived from strong-motion records can be easily detected and corrected by evaluating the correlation between the neighbouring stations.

2 METHODOLOGY

According to physics, low-frequency seismic signals at neighbouring stations should be coherent if the interstation distance is much smaller than the distance to the earthquake fault. Based on previous experience with the 2011 earthquake (Wang *et al.*, 2013), a dense strong-motion network normally contains stations that express (i) a negligible baseline shift (Fig. 2a) or (ii) a simple baseline shift with little or no transient interval (Fig. 2b). Records at these stations, which we call *elite stations*, lead to similar displacement estimates using different baseline correction methods. These elite stations together form a *first-generation* frame of reference. We used these elite stations to optimize the bilinear baseline correction for the neighbouring stations whose baseline shifts are more complicated. As a criterion, we required the corrected velocity seismograms to become as coherent as possible with those of the elite station reference. This allowed us to create an updated reference ('*second generation*'), and we could iterate this process further. In the following sections, we introduce this augmentation net-based algorithm.

2.1 Selection of reference records

We first made a preliminary baseline correction on the whole strong-motion data set using the empirical approach described by Wang

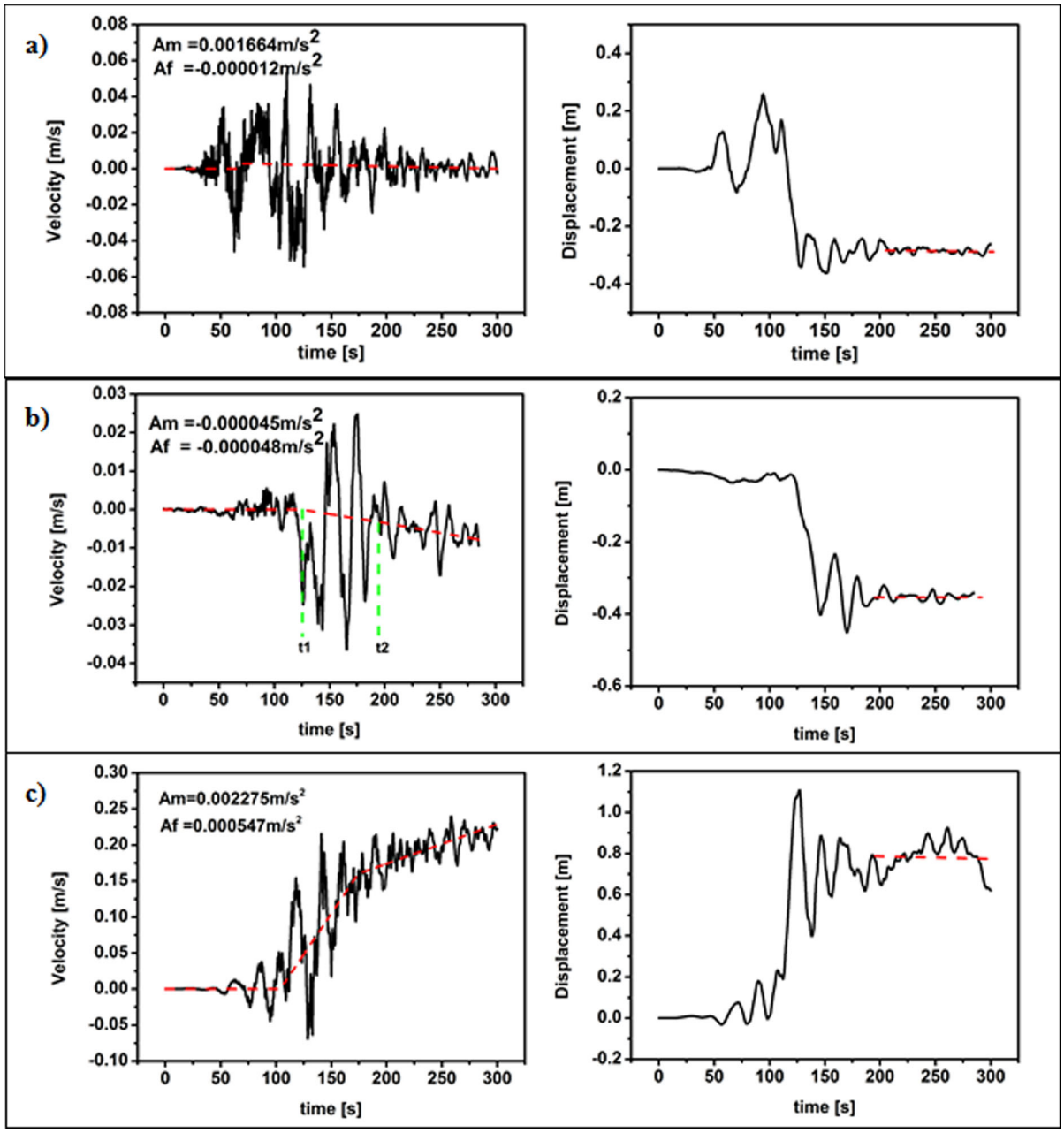

Figure 2. Examples of recovering velocity and displacement seismograms from strong-motion acceleration records. The red dashed lines are estimated velocity trends caused by baseline shifts in acceleration. The displacement seismograms are obtained by integrating the baseline corrected velocity seismograms. Three cases are shown: (a) negligible, (b) instantaneous and (c) complex baseline corrections. The data used in the three examples are from three borehole sensors of KiK-Net stations AKTH01 (vertical component), AICH06 (vertical component) and CHBN11 (east component), located at epicentral distances of 226, 630 and 391 km, respectively.

et al. (2011) and selected some of the elite stations to define the first-generation reference. In our approach, these reference records were selected based on the following two criteria:

(1) The record must have a stable post-event displacement record. In our study, this criterion is satisfied if the root-mean-square (rms) deviation of the displacement in the post-event time window (t_3 to t_e) is below a given threshold (we used 2 cm from experience).

(2) The second criterion is that the transient baseline shift between the pre- and post-event should be either negligible or an instantaneous step. In the former case, the final displacement is not significantly dependent on the selection of the timing parameters t_1 and t_2. In the latter case, although the baseline shift is significant, it can be robustly corrected because of its instantaneous offset. In such a case, the deviations in the final displacement should not exceed a given threshold (in this study, we used both the relative threshold of 10 per cent and the absolute threshold of 10 cm) to compare different empirical baseline correction schemes.

As an elite station should show at least a very stable post-event baseline offset, we chose the threshold for the post-event displacement fluctuation (criterion 1) to be considerably smaller than the expected uncertainty of the retrieved displacement. The total number of qualified reference stations from a network is mainly dependent

on the threshold used in criterion 2. The reference threshold should be as large as necessary to ensure that enough references cover the network area. This threshold will roughly reflect the lower bound of the standard uncertainties of the strong-motion derived displacement using the present method. Fig. 2 shows three examples for the strong-motion derived velocity and displacement seismograms with the baseline shift determined by the empirical method discussed in Wang *et al.* (2011). Fig. 2(a) shows a stable baseline, Fig. 2(b) shows an instantaneous baseline shift and Fig. 2(c) shows large and complex baseline variations. While the first two examples qualify as first-generation references according to the criteria, the third does not.

2.2 Net-based correction on target records

We calculated the east, north and vertical components of the velocity's cross-correlations between all remaining records and the first-generation reference records. Here, a low-pass ($\leq$1.0 Hz, for example) filter was applied to the data before calculating correlations to limit the influence from local effects. No significant difference was observed when a smaller cut-off frequency for the low-pass filter was chosen, likely because the velocity waveform at a frequency band higher than 0.1 Hz is generally not affected by baseline errors (Boore 2001). We selected one of the remaining records whose correlation coefficient to a neighbouring reference was the largest and was larger than 0.5. A neighbouring station is not necessarily the nearest station but any one from a neighbourhood with a radius one to two times larger than the average interstation distance of the network. The selected record is called the target record, whose baseline shift will be re-determined using our new net-based scheme. We selected t_1 and t_2 such that the correlation between the corrected velocity history of the target record and that of the reference record is maximized. After this net-based baseline correction, the target record became a next-generation reference and was used for subsegment target records. After the iterative augmentation, there may be remaining records for which no appropriate reference record can be found. This occurs mostly when either the concerned component of the strong-motion sensor indicates problems in the measurement system or when the nearest station is far away (violating the dense network condition). In the latter case, the station-independent approach needs to be used for the baseline correction.

2.3 Detection of outlier records

During each iteration previously discussed, we compared the correlation coefficient to identify how successful the new (i.e. target) correlation effort was. The aim was to identify those records that behaved randomly or that did not have a specific degree of similarity to the neighbouring reference station. Based on the existing reference records, we estimated the maximum spatial gradient of the final displacement field within the network using a quadratic polynomial regression. If the final displacement derived from the target record was not abnormal compared to the value expected from the spatial gradient, the net-based baseline correction was considered successful, and the corrected target record became a new reference record. Otherwise, the net-based baseline correction was considered a failure for this target record. In the latter case, the preliminary empirical baseline correction was retained but was flagged as having an unknown uncertainty. This procedure was repeated until the whole data set was processed or no target record with enough correlation to the reference could be identified. The outliers are those records that do not fulfill the correlation criterion and that are not treated as second-order (or higher order) reference records. These records are either excluded from our further analysis or are coming from sites accommodating local effects that may be further investigated.

3 APPLICATION TO STRONG-MOTION DATA FOR THE 2011 M_W 9.0 TOHOKU EARTHQUAKE

To validate the new, net-based baseline correction scheme, we tested it on the strong-motion data from the 2011 Tohoku earthquake and compared the results with GPS data and with the results obtained using previous empirical correction schemes.

3.1 Data

In this test, we used the strong-motion data from 417 K-Net and 266 KiK-Net stations (Aoi *et al.* 2004). Each of the KiK-Net stations are equipped with both surface and borehole sensors. In addition, the post-processed solutions from 414 GEONET GPS stations (Miyazaki *et al.* 1998) were explored to compare and validate our net-based strong motion correction scheme (Fig. 3). The KiK-Net stations are mostly installed on hard rocks, while the K-Net stations are mainly located in public buildings and schools for rapid response purposes. Therefore, the KiK-Net station's data quality (signal-to-noise ratio, baseline errors, etc.), particularly their borehole sensors, is expected to be higher than that of the K-Net stations. The interstation distances between the KiK-Net stations and K-Net stations are approximately 20 and 15 km, respectively, which is approximately one order smaller than the smallest epicentral distance to the two networks. Thus, we believe that the present case is appropriate for our net-based baseline correction scheme. Below, we classify the available strong-motion records into nine data subsets, three each for the borehole KiK-Net (borehole), surface KiK-Net (surface) and K-Net, respectively, each with east, north and vertical components. The three subsets of each data set contain initial reference stations, subsegment reference stations and errant stations.

3.2 Selected reference records

We first performed a preliminary baseline correction for the whole data set using the empirical scheme by Wang *et al.* (2011) and then selected the initial reference records for each of the nine data subsets according to the criteria discussed in the previous section (Table 1). This step yielded more reference records in the KiK-Net (borehole) than in the KiK-Net (surface) and the fewest in the K-Net records. The reference records found in all nine data subsets were scattered broadly within the corresponding networks (Fig. 4).

To validate the methods, coseismic static displacements derived from the reference strong-motion records were compared to the interpolated GPS displacements, which we derived based on the source model inverted from the GPS data (Wang *et al.* 2013). The results of this comparison are shown in Fig. 5. The standard deviations of the coseismic static displacements derived from the reference strong-motion records ranged from 13 to 27 cm for the nine data sets. These deviations can be regarded as the uncertainties of the displacement data derived from the reference strong-motion records. The deviations are not dramatically different from the threshold (10 per cent relatively and 10 cm absolutely) that we used to select the first-generation references. The uncertainties can be reduced if we tightened the criteria of the reference selection.

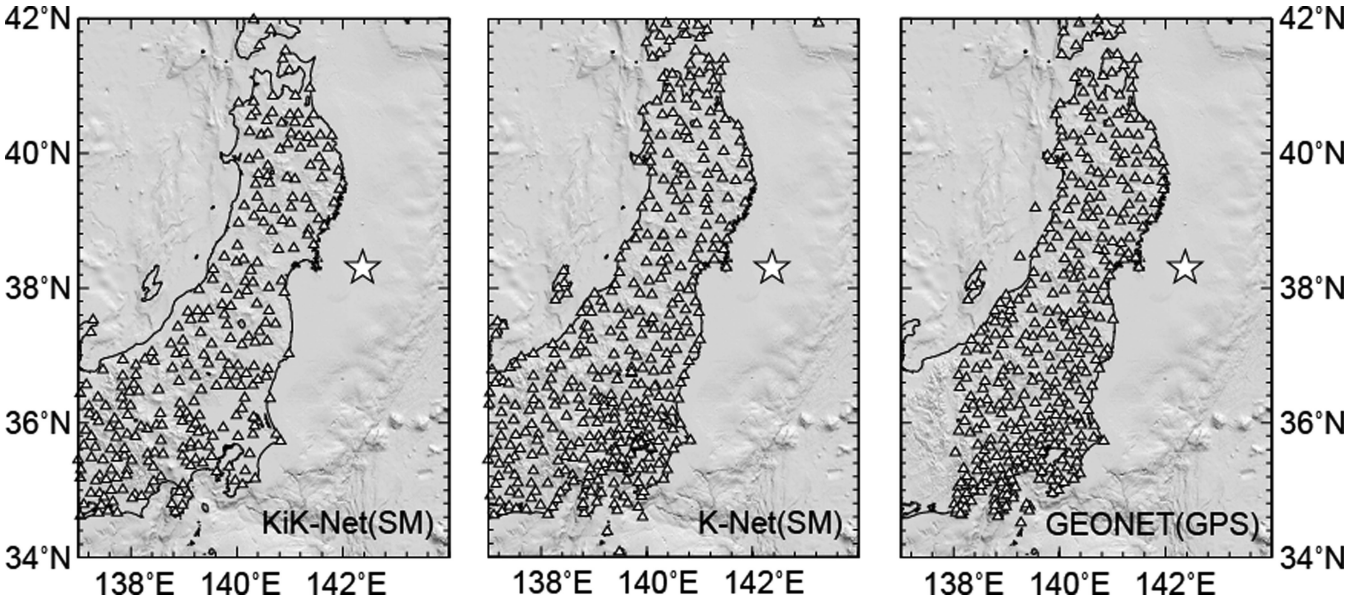

Figure 3. The distribution of the networks. Left, a map of the strong-motion network KiK-Net. Middle, a map of the strong-motion network K-Net. Right, a map of the GPS network GEONET. The white star in each panel is the epicentre of the 2011 Tohoku earthquake.

Table 1. Percentages of first-generation reference, target and outlier records in the different subsets of data used in this study.

Network	No	Reference (per cent)			Target (per cent)			Outlier (per cent)		
		East	North	Up	East	North	Up	East	North	Up
KiK-Net (borehole)	266	58.3	62.8	70.3	25.9	29.7	25.2	15.8	7.5	4.5
KiK-Net (surface)	266	49.6	57.9	66.9	24.1	29.7	26.7	26.3	12.4	6.4
K-Net	417	37.6	35.0	43.6	24.1	42.5	44.9	38.3	22.5	11.5

This would, however, lead to an insufficient coverage of the reference records.

3.3 Augmented target records

We improved the baseline correction using the net-based scheme for the records that were first disqualified as references. This procedure was performed for each of the nine data subsets. The records with a maximum correlation to one of the existing reference records in its neighbourhood (i.e. within a 30 km radius in the present case) were selected. This procedure was repeated until the entire data subset was processed. Records with a maximum correlation below the given threshold (we used 0.5 from experience) were defined as outliers. The number of 'good' stations was reduced, leaving us with typically more than three out of four stations. Of the available waveforms, the target records with waveform correlation coefficients greater than 0.5 compared to their neighbouring reference were approximately 93 per cent for the KiK-Net (borehole) data, 86 per cent for the KiK-Net (surface) data and 76 per cent for the K-Net data (Fig. 6).

After the net-based baseline correction, coseismic static displacements were derived from the target records, and the results were evaluated against 'GPS displacement'. The histograms in Fig. 7 show that the standard deviations of our results were reduced by 30–50 per cent compared to the results using the previous empirical approach. In particular, the most significant improvements were achieved for the three K-Net data subsets. This result adds considerably to the data available for analysing earthquake displacement. It was previously believed that the static displacement could not be retrieved from the K-Net records (Wang *et al.* 2011).

3.4 Outlier records

In our net-based approach, outlier records were those that had an insufficient correlation to their neighbouring reference, either for the waveform or for its estimated static displacement. The threshold we used for the waveform correlation was 0.5, and the maximum allowed interstation deviation in displacement was 40 cm (determined by analysing the whole network) for all nine subdata sets. For our interstation distance of approximately 10–20 km, the 40 cm threshold in the displacement between neighbouring stations corresponds to a maximum coseismic strain on the order of 10^{-4}–10^{-5}.

As expected, outlier records are detected more often in data from the K-Net than from the KiK-Net (Table 1). Fig. 8 shows the deviations of the displacements derived empirically from the outlier records in the nine subdata sets. The standard deviations ranged from 29 to 49 cm, which is much larger than that for the reference records. This implies that no stable information for the displacement can be retrieved from these outlier strong-motion records by seismic-only methods, including the present one.

3.5 Improvements over the previous empirical approaches

Compared to the results obtained using the empirical approach of Wang *et al.* (2011), the present net-based approach generally improves the consistency of the derived coseismic displacements with

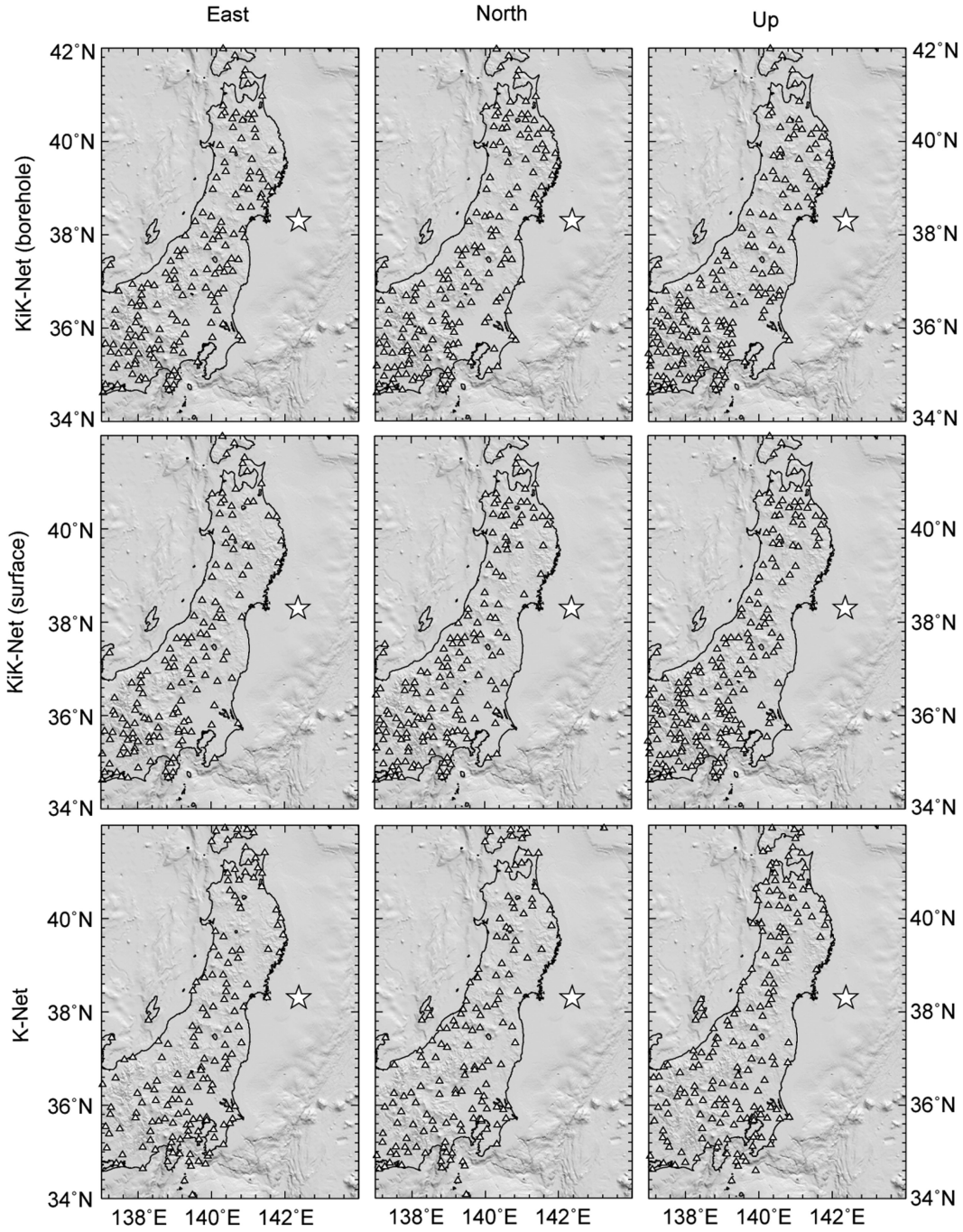

Figure 4. Spatial distribution of the first-generation reference records in the nine subdata sets. From top to bottom: KiK-Net (borehole), KiK-Net (surface) and K-Net; from left to right: the east, north and vertical components.

'GPS displacements' (Fig. 9). Using our approach, the most significant improvements were achieved for the K-Net data subsets. In Fig. 10, we compare the net-based approach to other approaches by comparing deviations in the rms to the corresponding GPS measurements. Depending on the data subsets used, the net-based approach was found to reduce the rms deviations by 20–43 per cent. Deleting all of the automatically detected outliers further improves the rms deviations by another 5–30 per cent. We combined a complete set of the displacement vectors derived from all the three strong-motion networks, which is shown in Fig. 11. This figure shows that the net-based approach leads to coherent spatial variations of strong-motion-based displacement. Compared to the results obtained by Wang *et al.* (2013), the station-independent empirical approach greatly improved through the net-based approach, particularly for the K-Net sites.

For some strong-motion stations, the data allow a direct comparison with the GPS measurements at a nearby site. Wang *et al.* (2013) showed that the displacement seismograms derived from records of the KiK-Net borehole sensors are consistent with the nearby GPS time-series. To demonstrate the efficacy of our net-based approach, we choose the north–south component recorded by the KiK-Net station IWTH23 surface sensor (116 km from the epicentre). It is representative, has KiK-Net station IWTH27 located approximately 17 km away and is selected as the reference station. In Fig. 12, the

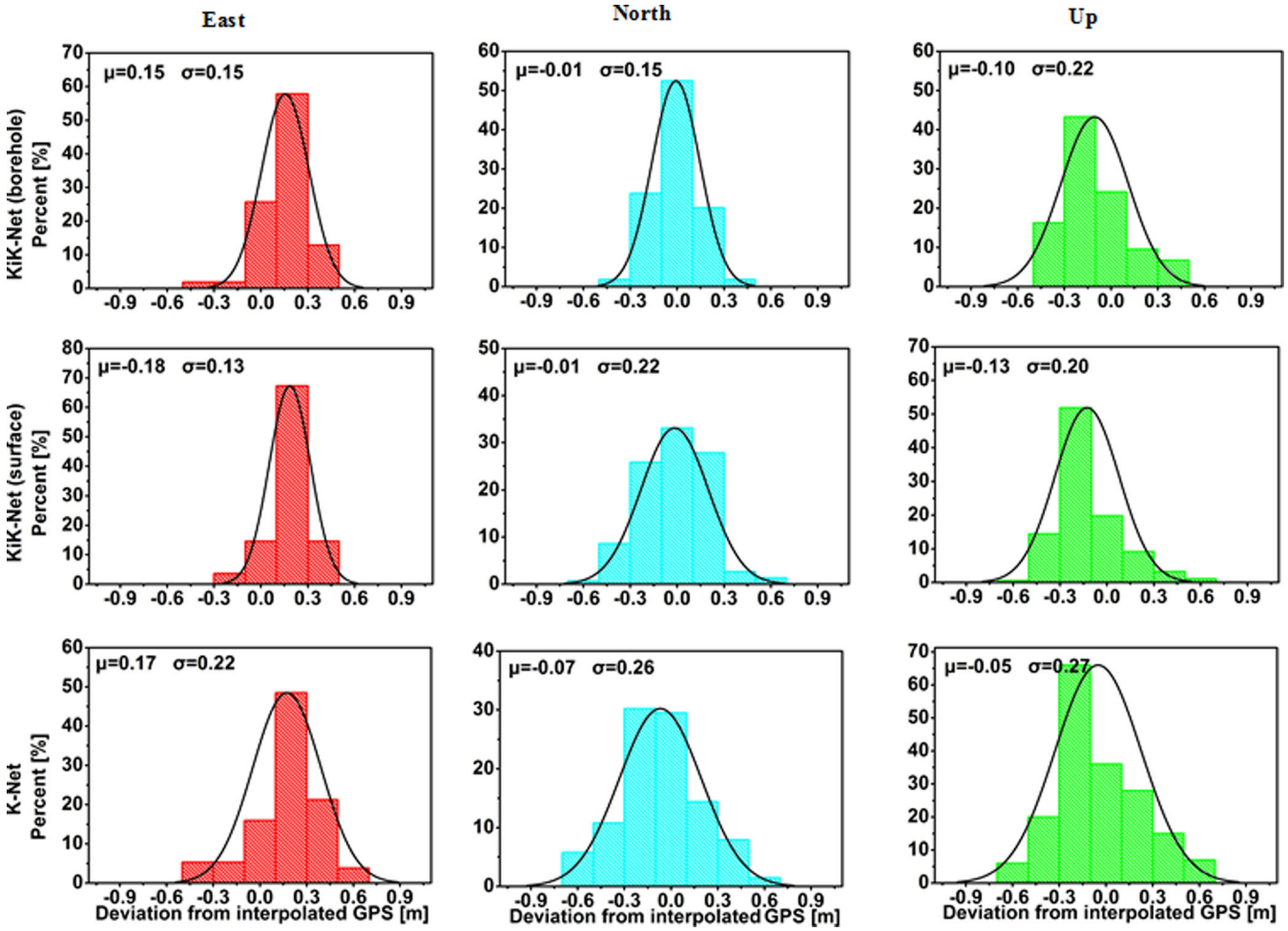

Figure 5. Histograms of the deviation of coseismic static displacements derived from the reference strong-motion records. The solid curves are the best-fit Gaussian distributions with mean deviation μ and standard deviation σ. From top to bottom: KiK-Net (borehole), KiK-Net (surface) and K-Net; from left to right: the east, north and vertical components.

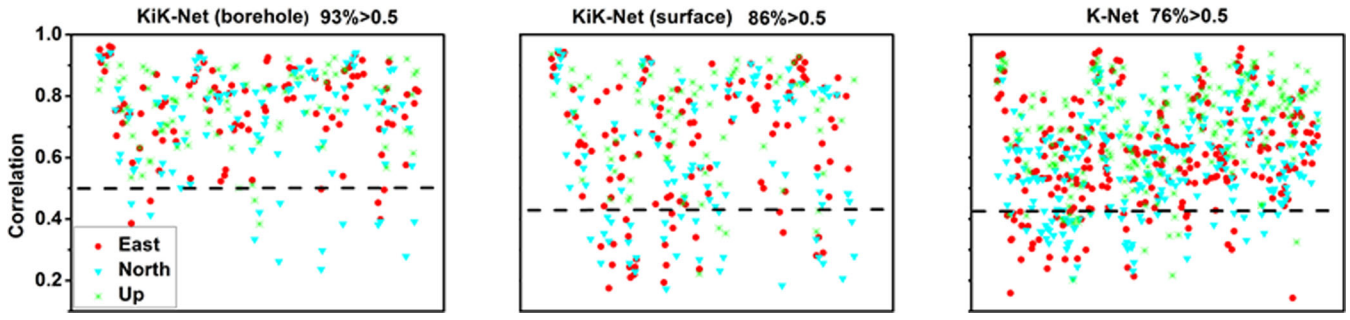

Figure 6. Maximum correlation coefficients between all target records and their first-generation reference records (both filtered by a low-pass filter of 1.0 Hz) in the different subdata sets.

bilinear correction of the raw velocity seismogram and the corrected velocity seismograms obtained using the net-based method are compared with those using two empirical methods. We also show the results of the reference station IWTH27 (Fig. 12) and found no significant difference between different baseline correction methods. For station IWTH23, however, the improvements from our net-based method are significant compared to the net-independent methods; the bias of coseismic displacement was reduced from 2.5 to 0.3 m. High-rate (1 sps) GPS seismograms are available from a nearby station, GEONET-0170, 3.2 km away from IWTH23. Fig. 13 shows the deviations (black curve) of the strong-motion-integrated velocity seismogram (without baseline correction) from the GPS velocity seismogram and different bilinear baseline corrections (colour lines). We believe that this deviation seismogram represents the true baseline errors in the strong-motion data, including both transient and permanent displacements. The net-based baseline correction fits the deviation seismogram considerably better than the two station-independent baseline corrections.

In the current net-based approach, the reference station selected for IWTH23 is IWTH27 which is 17.0 and 16.2 km away from IWTH23 and Geo-Net-0170, respectively. Fig. 14 shows a comparison of ground velocity spectra obtained by different approaches.

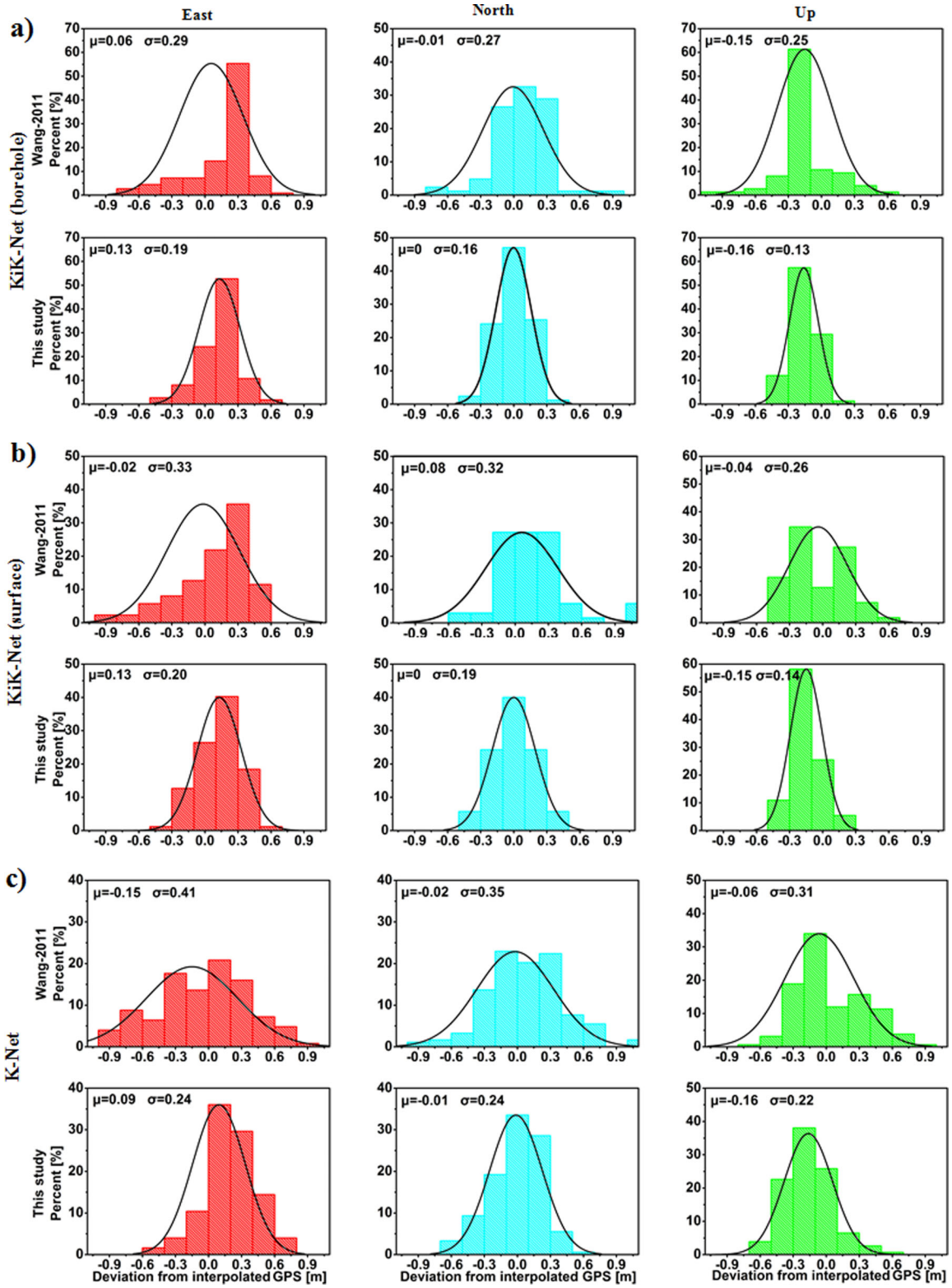

Figure 7. Histograms of the deviation of coseismic static displacements derived from the target records using the net-based baseline correction method compared with those using the previous net-independent method. The solid curves are the best-fit Gaussian distributions with mean deviation μ and standard deviation σ. From a to c: KiK-Net (borehole), KiK-Net (surface) and K-Net; from left to right: the east, north and vertical components.

Because of the negligible baseline shift of the accelerometer at IWTH27, the strong-motion derived velocity spectrum at this station agrees with the corresponding GPS spectrum at Geo-Net-0170 particularly in the low-frequency band up to 0.04 Hz. The differences at higher frequencies may be attributed to site effects. For IWTH23, though the accelerometer exhibited a complex baseline variation, the strong-motion derived velocity spectra are significantly different for the different baseline correction approaches

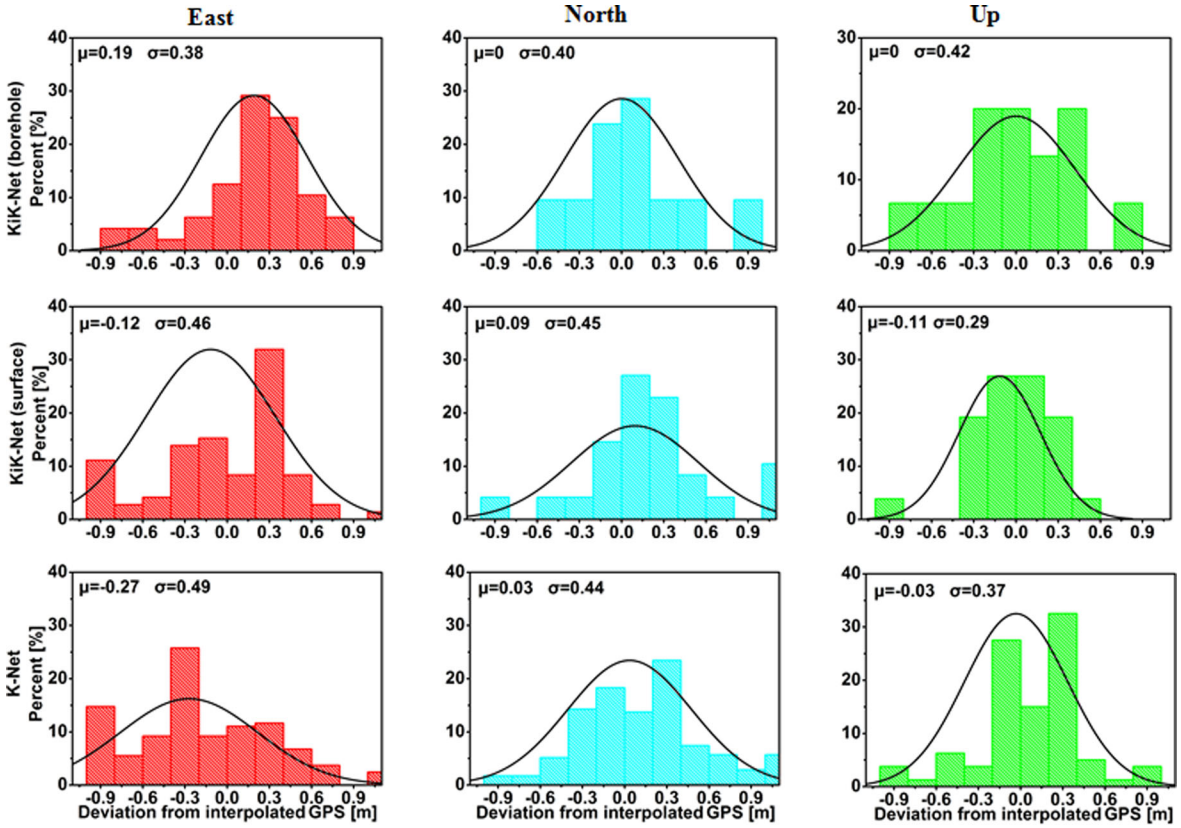

Figure 8. Histograms of the deviation of strong-motion derived coseismic displacements detected in this study as outliers. The solid curves are the best-fit Gaussian distributions with mean deviation μ and standard deviation σ. From top to bottom: KiK-Net (borehole), KiK-Net (surface) and K-Net; from left to right: the east, north and vertical components.

only at very low frequencies ($\leq$0.02 Hz in this case), confirming the observation by Boore (2001). In comparison, the result by the net-based baseline correction approach agrees considerably better with the GPS in the low-frequency band than the station-independent approach.

4 CONCLUSION AND DISCUSSION

In this study, we proposed a net-based scheme for baseline corrections of digital strong-motion records, in which we assumed that the seismic waveforms at neighbouring stations should generally be coherent. In this scheme, the pre-event and post-event baseline shifts are estimated using the criteria suggested by Wang *et al.* (2011), but the time window for the transient baseline shift (t_1, t_2) is selected so that the waveform correlation to the neighbouring reference station (whose baseline is good or can be corrected easily) is maximized. The net-based approach is able to detect records with large and complicated baseline shifts, those that cannot be easily approximated by a bilinear function.

We applied our new approach to all strong-motion data from the KiK-Net (both borehole and surface sensors) and K-Net (surface sensor) networks for the 2011 Tohoku earthquake. Compared to the previous results based on the station-independent baseline correction schemes, the net-based approach reduced the rms uncertainties of derived displacement records by as much as 50 per cent (Fig. 10).

In principle, the net-based approach requires a dense strong-motion network. We propose to apply the net-based approach to only those neighbouring stations whose low-pass filtered strong-motion records show sufficient correlations (e.g. $>$0.50). We make three primary conclusions:

1. The selection of the reference stations is crucial to our network solution. A statistical analysis of the pre-processed data is useful to optimize the selection criterion. In general, the first iteration reference stations should be distributed more or less randomly within the network. We need at least 30 per cent of the KiK-net and K-net data sets for the first iteration references.
2. To avoid the influence of the high-frequency incoherent signals associated with local structures and shallow nonlinear elasticity, the correlation among the neighbouring stations needs to be evaluated using low-pass filtered strong-motion records. Non-reference stations should be added iteratively in order of their correlation with existing nearby reference stations.
3. Detecting the outlier records is the most useful function of the net-based approach. Although the percentage of the outliers can reflect the overall quality of whole-network results, the outliers may indicate installation or recording problems at the instrument. Wang *et al.* (2013) discussed that the earthquake source can be resolved much better by removing the outliers from the data. Compared to the model-based outlier detection method suggested by Wang *et al.* (2013), our net-based detection approach does not need any prior knowledge of the earthquake source.

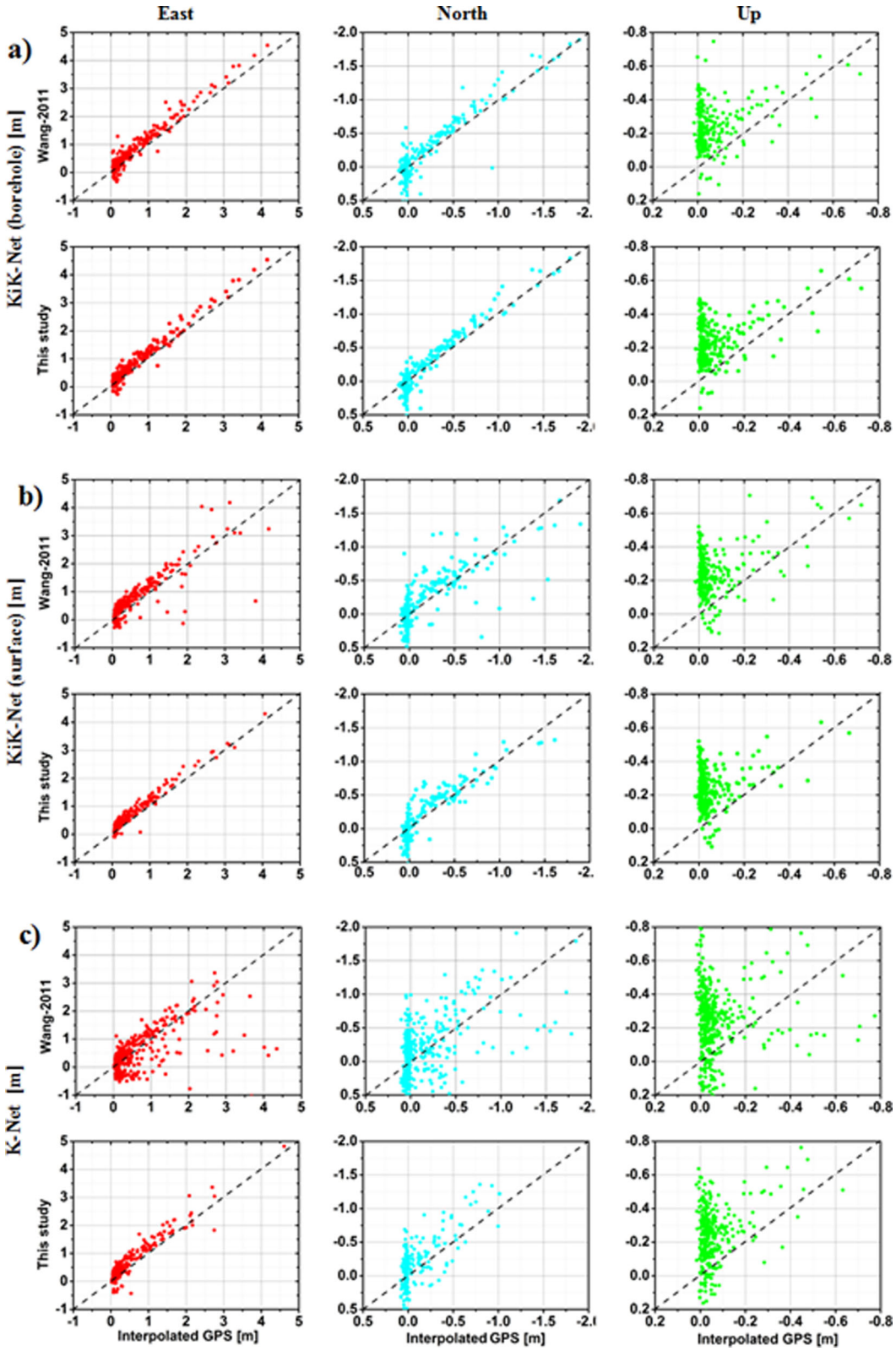

Figure 9. Comparison of strong-motion derived three-component coseismic displacement data with the (interpolated) GPS measurements. (a) KiK-Net (borehole) data, (b) KiK-Net (surface) data and (c) K-Net data.

In summary, using the net-based approach presented here, a robust, largely automatic recovery of coseismic displacement and low-frequency waveform data from strong-motion records is possible for most stations. Additionally, the method provides valuable input for seismology and earthquake early warning purposes. On the other hand, however, the common limitation of all seismic-only approaches including the present net-based one is also obvious. In particular, the strong-motion derived coseismic static displacement

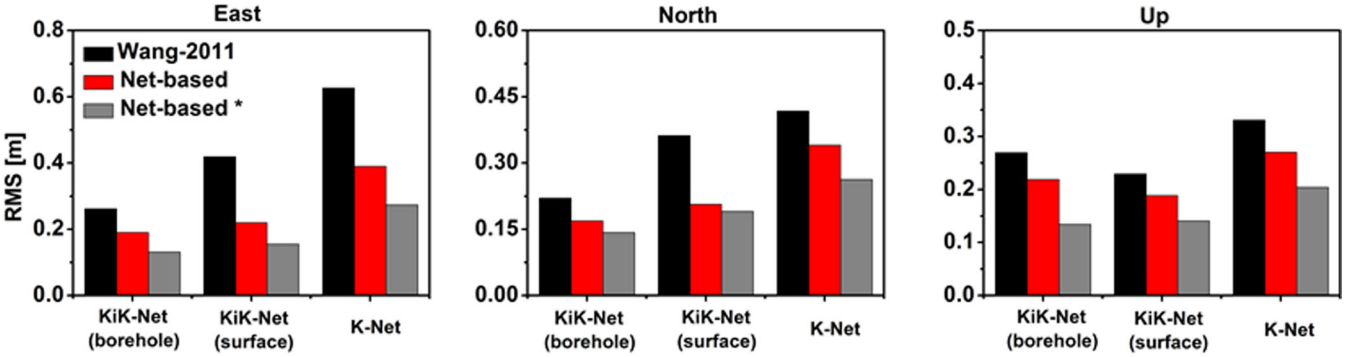

Figure 10. The rms deviations of the nine data subsets of strong-motion derived coseismic displacements for the Tohoku earthquake using different baseline correction approaches compared to the (interpolated) GPS measurements. Net-based* (grey) denotes the net-based results without the outliers.

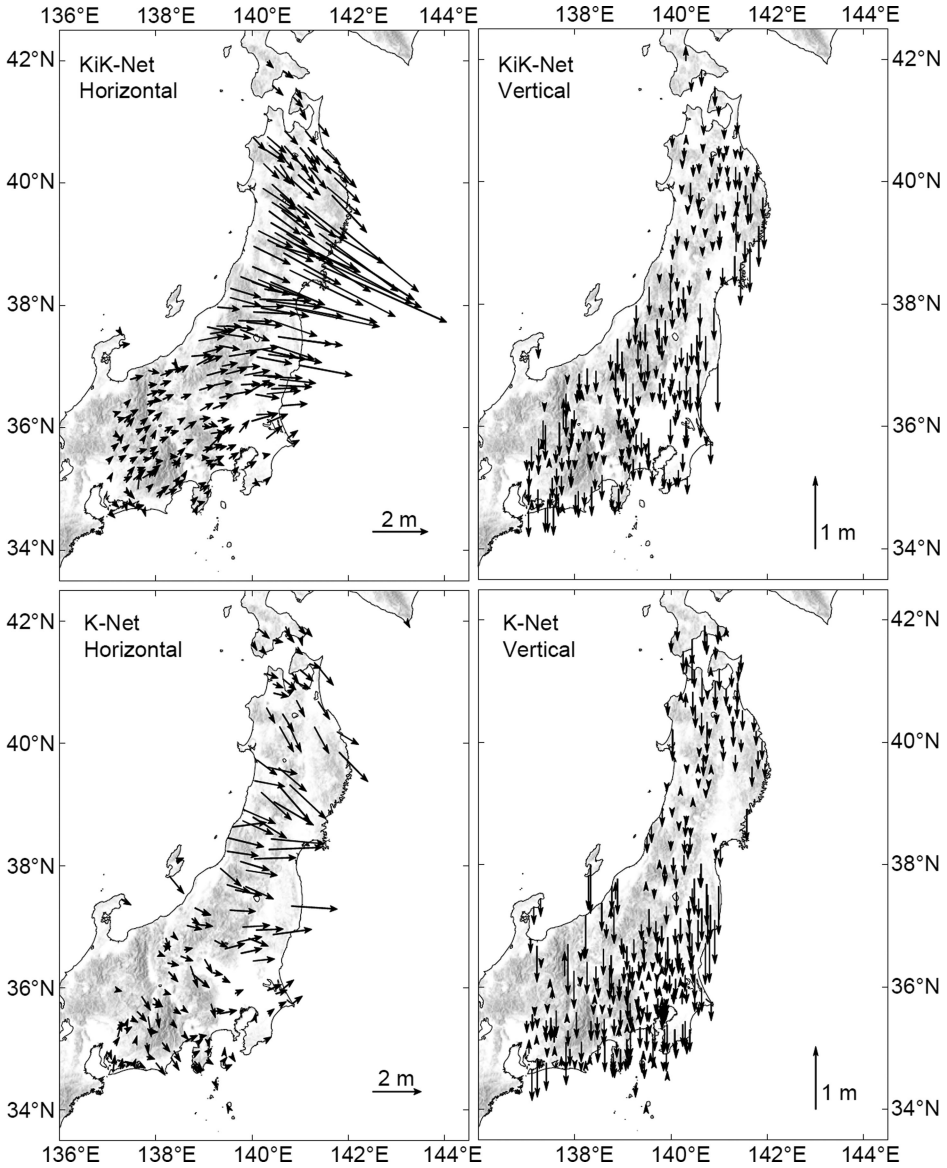

Figure 11. Coseismic displacement data set derived from the KiK-Net (top) and K-Net (bottom) strong-motion networks for the 2011 Tohoku earthquake. Stations for which only one horizontal component could be derived successfully are not plotted. If the KiK-Net data were available from both borehole and surface sensors, only the borehole result is shown.

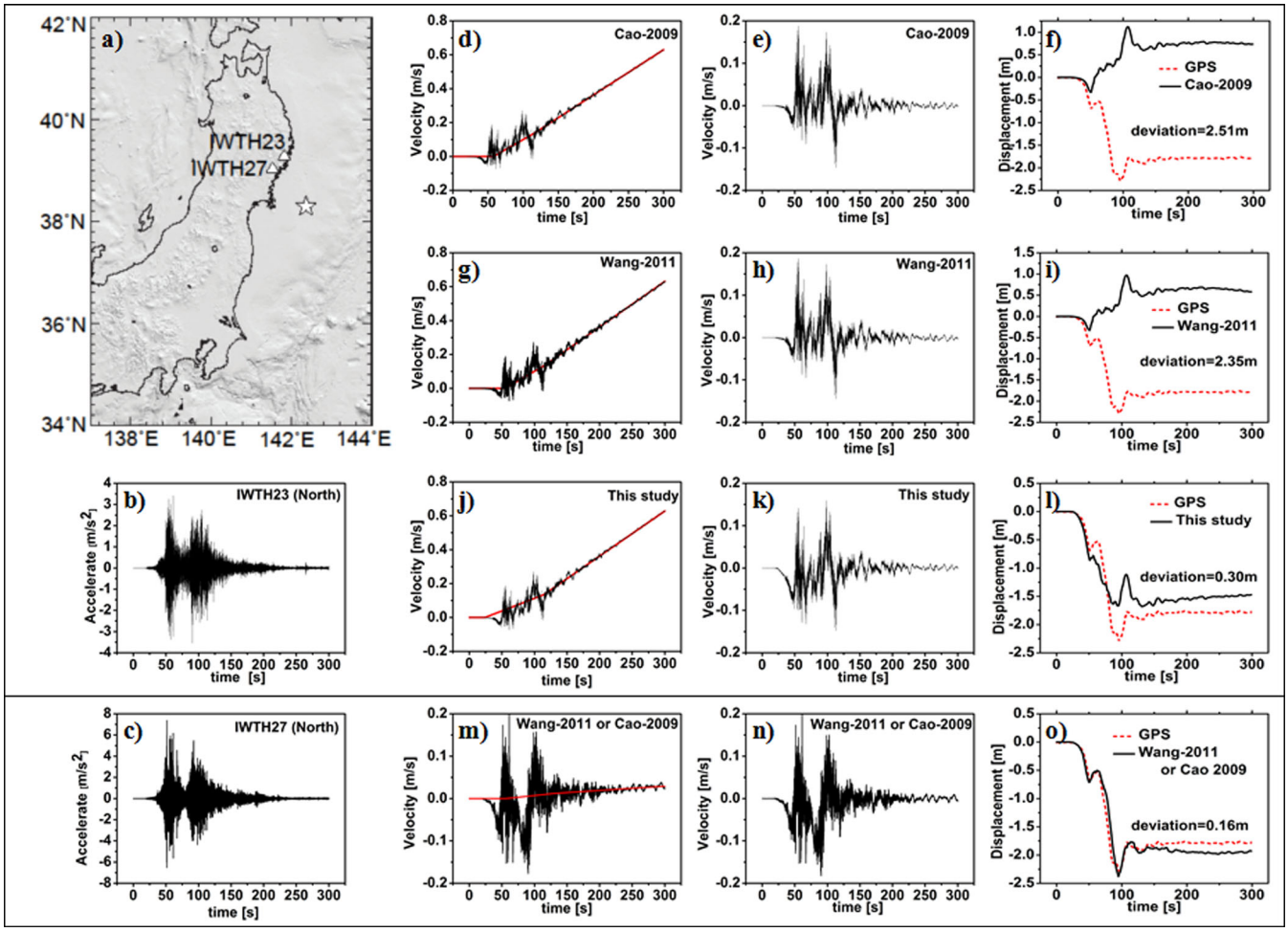

Figure 12. (a) Sitemap of KiK-Net stations IWTH23 and IWTH27. (b–c) Raw strong-motion records for stations IWTH23 and IWTH27 (N-S component). (d) Velocity seismogram (black curve) integrated from IWTH23 acceleration records, and the bilinear baseline correction (red line) determined using the method discussed by Chao *et al.* (2009). (e–f) Corrected velocity and displacement seismograms using the method described by Chao *et al.* (2009). (g–i) Same as (d–f) but using the method described by Wang *et al.* (2011). (j–l) Same as (d–f) but using our net-based method with IWTH27 as the reference station. (m–o) Same as (d–f) but for station IWTH27 and using the Chao *et al.* 2009 or Wang *et al.* (2011) method. The red dashed lines are GPS coseismic displacements for reference.

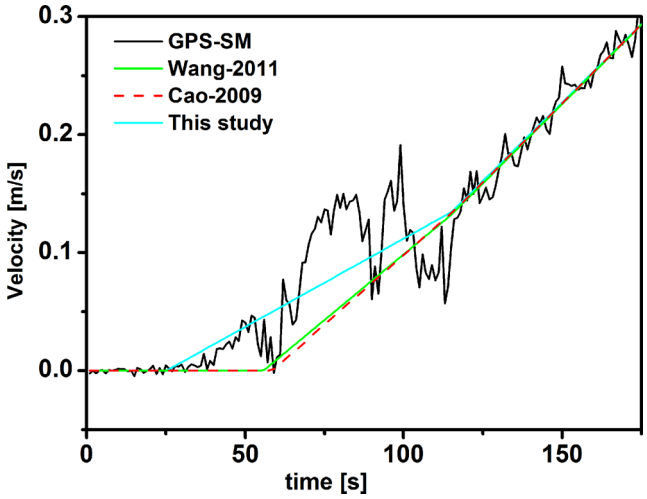

Figure 13. The black curve shows the deviations between the velocity seismograms integrated without correction from the record at KiK-Net station IWTH23 (NS component of the surface sensor) and differentiated GPS data at the nearby Geo-Net-0170 station. The coloured lines are various bilinear baseline corrections obtained using different methods as shown.

data still show large uncertainties. As the baseline shift is mainly caused by the simultaneous tilting and rotational motion of the ground, recovering the coseismic point ground tilt from collocated high-rate GPS and accelerometers is more useful and should play an important role for seismological developments in the near future (Geng *et al.* 2013b).

ACKNOWLEDGEMENTS

K-Net and KiK-Net strong-motion data for the 2011 Tohoku earthquake were provided by the National Research Institute for Earth Science and Disaster Prevention (NIED) of Japan and are available at http://www.k-net.bosai.go.jp/ and http://www.kik.bosai.go.jp/. All original GEONET GPS data were provided by the Geospatial Information Authority (GSI) of Japan. GPS coseismic displacement data produced by the ARIA team at JPL and Caltech were downloaded from ftp://sideshow.jpl.nasa.gov/pub/usrs/ARIA/. High-rate GPS data [of the GSI via Nippon GPS Data Services Company (NGDS)] were from http://rtgps.com/rtnet_dl_eq.php. Mr Rui Tu is supported by the China Scholarship Council for his Ph.D. study in Germany.

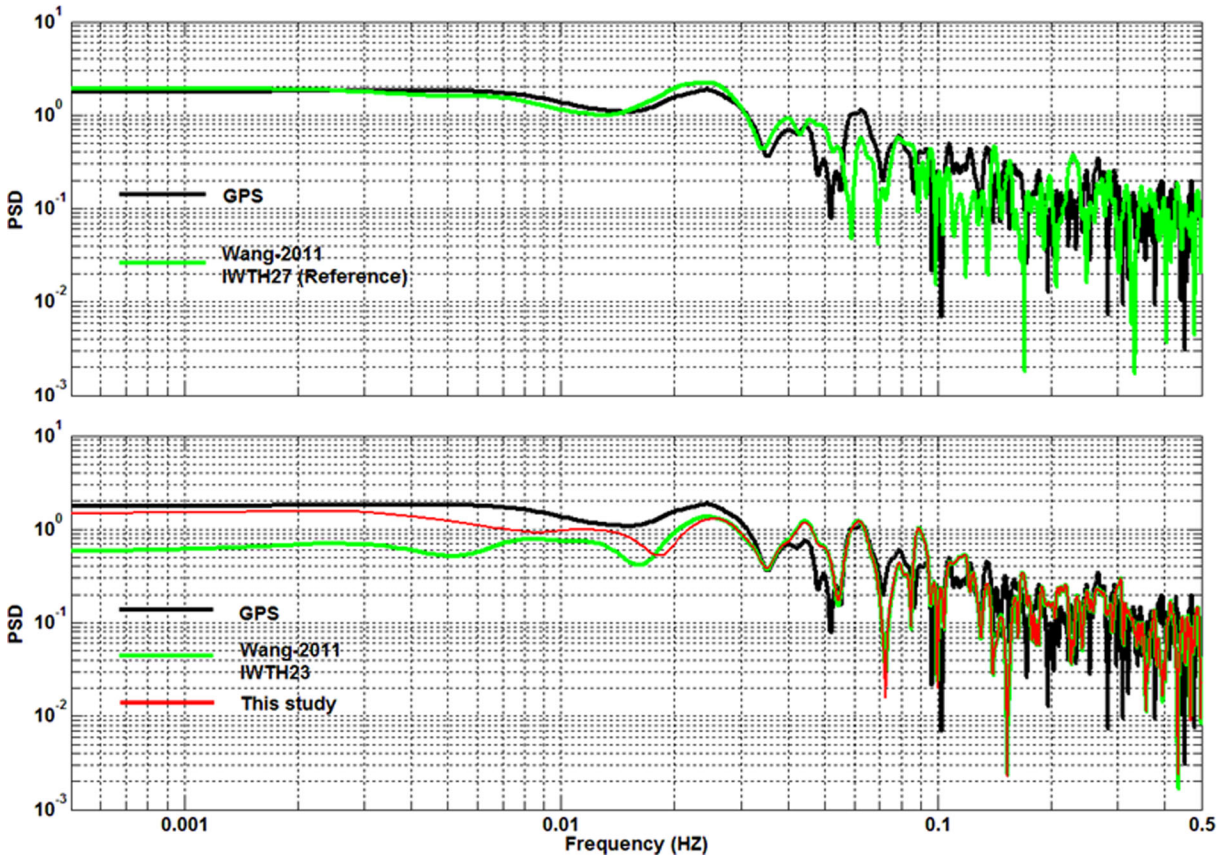

Figure 14. Fourier amplitude spectra of the ground velocity seismograms derived from strong-motion records at KiK-Net stations IWTH23 and IWTH27 (NS component of the surface sensor) compared with the corresponding spectra of the GPS at station Geo-Net-0170, which is 3.2 and 16.2 km away from the KiK-Net strong-motion stations IWTH23 and IWTH27, respectively. The distance between IWTH23 and IWTH27 is 16.2 km. In the present net-based baseline correction approach, IWTH27 is used as reference for IWTH23.

REFERENCES

Aoi, S., Kunugi, T. & Fujiwara, H., 2004. Strong-motion seismograph network operated by nied: K-Net and KiK-Net, *J. Japan Assoc. Earthq. Eng.,* **4,** 65–74.

Bock, Y., Melgar, D. & Crowell, B.W., 2011. Real-time strong-motion broadband displacements from collocated GPS and accelerometers, *Bull. seism. Soc. Am.,* **101,** 2904–2925.

Bock, Y. & Prawirodirdjo, L., 2004. Detection of arbitrarily large dynamic ground motions with a dense high-rate GPS networks, *Geophys. Res. Lett*., **31,** L06604, doi:10.1029/2003GL019150.

Boore, D.M., 2001. Effect of baseline corrections on displacement and response spectra for several recordings of the 1999 Chi-Chi, Taiwan, earthquake, *Bull. seism. Soc. Am.,* **91,** 1199–1211.

Chao, W., Wu, Y. & Zhao, L., 2009. An automatic scheme for baseline correction of strong-motion records in coseismic deformation determination, *J. Seismol.,* **14,** 495–504.

Chiu, H., 1997. Stable baseline correction of digital strong-motion data, *Bull. seism. Soc. Am*., **87,** 932–944.

Colombelli, S., Allen, R.M. & Zollo, A., 2013. Application of real-time GPS to earthquake early warning in subduction and strike-slip environments, *J. geophys. Res.,* **118,** 3448–3461.

Delouis, B., Nocquet, J.M. & Vallée, M., 2010. Slip distribution of the February 27, 2010 Mw = 8.8 Maule Earthquake, central Chile, from static and high-rate GPS, InSAR, and broadband teleseismic data, *Geophys. Res. Lett.,* **37,** L17305, doi:10.1029/2010GL043899.

Emore, G.L., Haase, J.S., Choi, K., Larson, K.M. & Yamagiwa, A., 2007. Recovering seismic displacements through combined use of 1-Hz GPS and strong-motion accelerometers, *Bull. seism. Soc. Am.,* **97,** 357–378.

Geng, J., Bock, Y., Melgar, D., Crowell, B.W. & Haase, S., 2013a. A new seismogeodetic approach applied to GPS and accelerometer observations of the 2011 Brawly seismic swarm: implications for earthquake early warning, *Geochem. Geophys. Geosyst.,* **14,** 2124–2142.

Geng, J., Melgar, D., Bock, Y., Pantoli, E. & Restrepo, J., 2013b. Recovering cosiesmic point ground tilts from collocated high-rate GPS and accelerometers, *Geophys Res. Lett.,* **40,** 5095–5100.

Graizer, V.M., 1979. Determination of the true ground displacement by using strong motion records, *Izv. Earth Phys.,* **25,** 26–29.

Graizer, V.M., 2005. Effect of tilt on strong motion data processing, *Soil Dyn. Earthq. Eng.,* **25,** 197–204.

Graizer, V.M., 2006. Tilts in strong ground motion, *Bull. seism. Soc. Am.,* **96,** 2090–2106.

Iwan, W., Moser, M. & Peng, C., 1985. Some observations on strong-motion earthquake measurement using a digital acceleration, *Bull. seism. Soc. Am.,* **75,** 1225–1246.

Irwan, M., Kimata, F., Hirahara, K., Sagiya, T. & Yamagiwa, A., 2011. Measuring ground deformations with 1-Hz GPS data: the 2003 Tokachi-oki earthquake (preliminary report), *Earth Planets Space,* **56,** 389–393.

Larson, K.M., Bodin, P. & Gomberg, J., 2003. Using 1-Hz GPS data to measure deformations caused by the Denali fault earthquake, *Science,* **300,** 1421–1424.

Li, X., Ge, M., Zhang, Y., Wang, R., Klotz, J. & Wicket, J., 2013. High-rate coseismic displacements from tightly-integrated processing of raw GPS and accelerometer data, *Geophys. J. Int.,* **195,** 612–624.

McComb, H.E., Ruge, A.C. & Neumann, F., 1943. The determination of true ground motion by integration of strong-motion records: a symposium, *Bull. seism. Soc. Am.,* **33,** 1–63.

Melgar, D., Bock, Y., Sanchez, D. & Crowell, B.W., 2013. On robust and reliable automated baseline corrections for strong motion seismology, *J. geophys. Res.,* **118,** 1171–1187.

Miyazaki, S., Tsuji, H., Hatanaka, Y. & Tada, T., 1998. The nationwide GPS array as an earth observation system, *Bull. Geogr. Surv. Inst.,* **44,** 11–22.

Nikolaidis, R.M., Bock, Y., Jonge, P.J., Shearer, P., Agnew, D.C. & Domselaar, M.V., 2001. Seismic wave observations with the global positioning system, *J. geophys. Res.,* **106,** 21 897–21 916.

Ohta, Y. *et al.*, 2012. Quasi real-time fault model estimation for near-field tsunami forecasting based on RTK-GPS analysis: application to the 2011 Tohoku-Oki earthquake (Mw 9.0), *J. geophys. Res.,* **117,** B02311, doi:10.1029/2011JB008750.

Salichon, J., Delouis, B., Lundgren, P., Giardini, D., Costantini, M. & Rosen, P., 2003. Joint inversion of broadband teleseismic and interferometric synthetic aperture radar (InSAR) data for the slip history of the Mw = 7.7, Nazca ridge (Peru) earthquake of 12 November 1996, *J. geophys. Res.,* **108,** 2085, doi:10.1029/2001JB000913.

Trifunac, M.D. & Todorovska, M.I., 2001a. A note on the useable dynamic range of accelerographs recording translation, *Soil Dyn. Earthq. Eng.,* **21,** 275–286.

Trifunac, M.D. & Todorovska, M.I., 2001b. Evolution of accelerographs, data processing, strong motion arrays and amplitude and spatial resolution in recording strong earthquake motion, *Soil Dyn. Earthq. Eng*., **21,** 537–555.

Tu, R., Ge, M., Wang, R. & Walter, T.R., 2014. A new algorithm for tight integration of real-time GPS and strong-motion records, demonstrated on simulated, experimental, and real seismic data, *J. Seismol.,* **18,** 151–161.

Tu, R., Wang, R., Ge, M., Walter, T.R., Ramatschi, M., Milkereit, C., Bindi, D. & Dahm, T., 2013. Cost effective monitoring of ground motion related to earthquakes, landslides or volcanic activities by joint use of a single-frequency GPS and a MEMS accelerometer, *Geophys. Res. Lett.,* **40,** 3825–3829.

Wang, R., Parolai, S., Ge, M., Jin, M., Walter, T.R. & Zschau, J., 2013. The 2011 Mw 9.0 Tohoku earthquake: comparison of GPS and strong-motion data, *Bull. seism. Soc. Am.,* **103,** 1336–1347.

Wang, R., Schurr, B., Milkereit, C., Shao, Z. & Jin, M., 2011. An improved automatic scheme for empirical baseline correction of digital strong-motion records, *Bull. seism. Soc. Am*., **101,** 2029–2044.

Wright, T.J., Houlié, N., Hildyard, M. & Iwabuchi, T., 2012. Real-time, reliable magnitudes for large earthquakes from 1 Hz GPS precise point positioning: the 2011 Tohoku-Oki (Japan) earthquake, *Geophys. Res. Lett.,* **39,** L12302, doi:10.1029/2012GL051894.

Wu, Y. & Wu, C., 2007. Approximate recovery of coseismic deformation from Taiwan strong-motion records, *J. Seismol.,* **11,** 159–170.

Zhu, L., 2003. Recovering permanent displacements from seismic records of the June 9, 1994 Bolivia deep earthquake, *Geophys. Res. Lett.,* **30,** 1740, doi:10.1029/2003GL017302.